Preprint Title	Radical reactivity of antiaromatic Ni(II) norcorroles with azo radical initiators
Authors	Siham Asyiqin Shafie, Ryo Nozawa, Hideaki Takano and Hiroshi Shinokubo
Publication Date	21 Mai 2024
Article Type	Letter
Supporting Information File 1	SI_radical_ver4.pdf; 1.1 MB
ORCID® iDs	Hideaki Takano - https://orcid.org/0000-0003-0744-9292; Hiroshi Shinokubo - https://orcid.org/0000-0002-5321-2205

Radical reactivity of antiaromatic Ni(II) norcorroles with azo radical initiators

Siham Asyiqin Shafie‡1, Ryo Nozawa‡1, Hideaki Takano,[1,2] and Hiroshi Shinokubo*1

Address: [1]Department of Molecular and Macromolecular Chemistry, Graduate School of Engineering and Integrated Research Consortium Chemical Sciences (IRCCS), Nagoya University, Nagoya, Aichi 464-8603, Japan and [2]Institute for Advanced Research, Nagoya University

Email: hshino@chembio.nagoya-u.ac.jp

* Corresponding author

‡ Equal contributors

Abstract

Norcorrole is a stable 16π antiaromatic porphyrinoid that exhibits characteristic reactivities and physical properties. Here, we disclose the reaction of Ni(II) norcorroles with alkyl radicals derived from azo radical initiators. The radical selectively attacked the distal α-position to the *meso* position to construct a non-aromatic bowl-shaped structure. The photophysical and electrochemical properties of the obtained radical adducts were compared with those of the parent Ni(II) norcorrole. The radical reactivity of Ni(II) norcorroles was investigated by density functional theory (DFT) calculations.

Keywords

porphyrinoid; norcorrole; antiaromatic; radical

Introduction

Considerable attention has been directed toward antiaromatic norcorroles[1–3] due to fascinating physical properties such as reversible redox properties[4,5] and stacked-ring aromaticity[6–10]. While Ni(II) norcorroles are stable under ambient conditions despite their distinct 16π antiaromaticity, they show unique reactivities to various reagents due to their high-lying HOMO and low-lying LUMO (Figure 1)[11]. The reactions with nucleophiles (Nu) proceed with perfect regioselectivity at the distal β-position to the *meso* positions[12–15]. On the other hand, the reactions with electrophiles (El) also undergo preferentially at the β-positions, but the regioselectivities depend on electrophiles[16–18]. In addition, C–C double bonds of the norcorrole skeleton on the outside of the π-delocalization pathway exhibit a similar reactivity to an alkene to afford hydrogenated norcorroles by hydrogenation[19] or reduction with hydrazine[20] and [3+2] cycloadducts with 1,3-dipoles[21]. Moreover, the ring-expansion or ring-opening reactions of Ni(II) norcorroles are induced by an activated zwitterionic intermediate[22], oxidants[23,24], and carbenes[25,26].

During the last decade, the various reactivities of Ni(II) norcorroles have been elucidated. However, the reaction with radical species has remained unexplored. Here, we disclose the radical functionalization of Ni(II) norcorroles with simple and frequently used azo radical initiators to furnish non-conjugated macrocycles with bowl-shaped structures[27]. The photophysical and electronic properties of obtained products are also presented. We also discuss the reaction selectivity of the radical addition to Ni(II) norcorroles using DFT calculations.

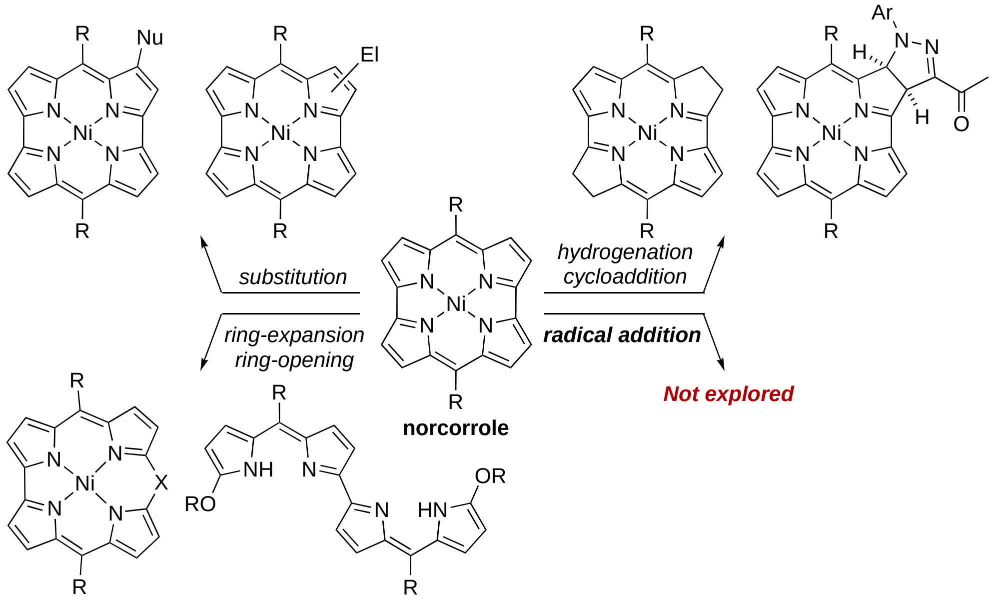

Figure 1: The reactivities of norcorroles with various reagents.

Results and Discussion

Reactivity with azo radical initiators

We selected 2,2'-azobis(isobutyronitrile) (AIBN) as a radical source. Ni(II) dimesitylnorcorrole **1** was treated with AIBN in toluene at 130 °C (Scheme 1). The reaction smoothly proceeded to afford dialkylated macrocycle **2a** in 92% yield. In addition to **2a**, monoalkylated product **3a** and dipyrrin dimer **4a** were obtained as minor products in 4% and 3% yields, respectively.

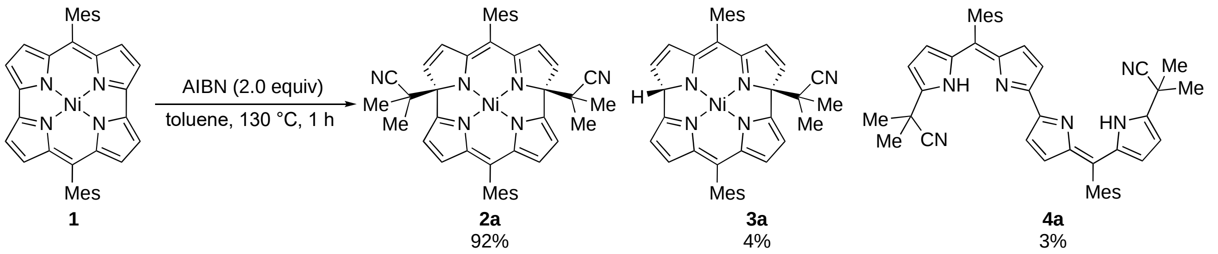

Scheme 1: Reaction of norcorrole **1** with AIBN.

The structure of **2a** was unambiguously confirmed by X-ray single crystal analysis, which exhibited that two alkyl substituents were located on the same side of the molecule (Figure 2a). Compared with the planar structure of **1** (Figure 2b)[2], **2a** displays a non-planar structure due to sp^3 carbon atoms adjacent to nitrogen atoms. The ^{1}H NMR spectrum of **2a** suggests that the radical addition reaction modified the antiaromatic norcorrole to the non-aromatic macrocycle (see Supporting Information).

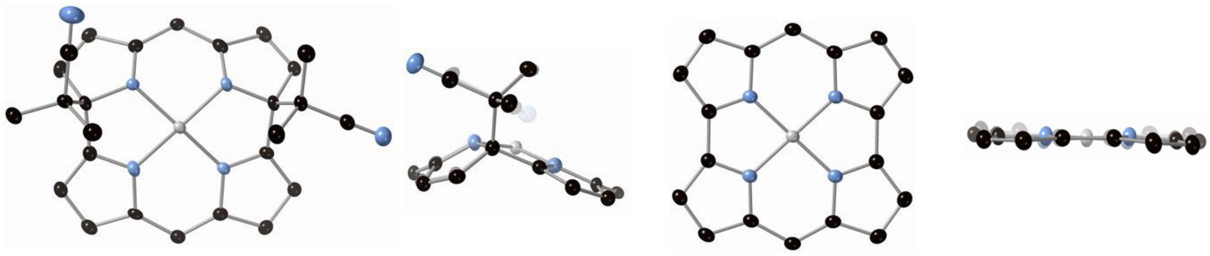

a) X-ray structure of **2a**

b) X-ray structure of **1**

Figure 2: X-ray structures of **2a** and **1**[2]. Mesityl groups and hydrogen atoms were omitted for clarity. Thermal ellipsoids are drawn at 50% probability.

1,1'-Azobis(cyclohexane-1-carbonitrile) (V-40) was also examined as a radical source. The reaction afforded **2b** in 87% yield (Scheme 2). Unfortunately, other radical sources such as benzoyl peroxide, TEMPO, and the combination of alkyl halides with BEt_3 were not applicable to this reaction.

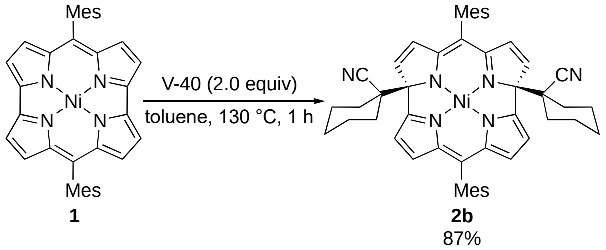

Scheme 2: Reaction of norcorrole **1** with V-40.

Physical properties

The electronic absorption spectra of norcorrole **1** and adduct **2a** are shown in Figure 3. While norcorrole **1** exhibited a weak absorption band from 600 nm to a NIR region, which was derived from the characteristic forbidden HOMO–LUMO transition of an antiaromatic compound, non-conjugated macrocycle **2a** did not have such absorption bands, indicating the loss of antiaromaticity in **2a**. Macrocycle **2a** possessed new absorption bands from 600 nm to 800 nm. The simulated absorption spectrum of **2a** by the TD-DFT calculation at the M06/6-31G(d)+SDD//B3LYP-D3/6-31G(d)+SDD level of theory was consistent with an experimental result, of which the longest absorption band was attributed to the transition from HOMO to LUMO+1 (670 nm, *f* = 0.0026).

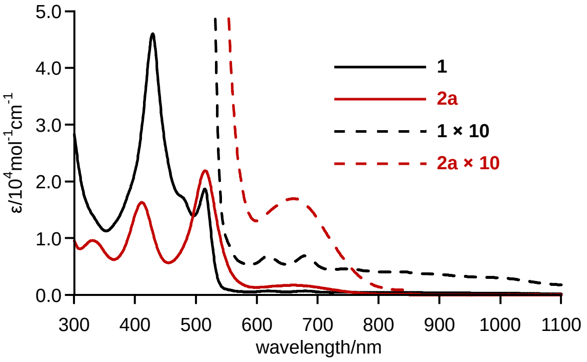

Figure 3: UV/vis/NIR absorption spectra of **1** and **2a** in CH_2Cl_2.

Next, the electrochemical property of **2a** in CH_2Cl_2 was examined using cyclic voltammetry (Figure 4). Macrocycle **2a** exhibited one reversible oxidation wave at 0.44 V and two reversible reduction waves at –0.85 V and –1.14 V. The electrochemical HOMO–LUMO gap of **2a** is 1.29 V, which is larger than that of **1a** (1.08 V)[2].

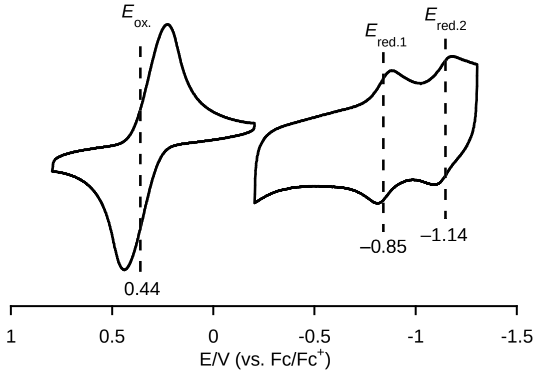

Figure 4: Cyclic voltammogram of **2a** in CH_2Cl_2. Supporting electrolyte: 0.1 M

Bu_4NPF_6; working electrode: glassy carbon; counter electrode: Pt; reference electrode: Ag/$AgNO_3$; scan rate: 50 mV s^{-1}.

DFT calculations

We next conducted DFT calculations using Gaussian 16[28] to elucidate the reactivity of Ni(II) norcorroles to radical species (Scheme 3). All calculations for the ground state were performed at the (U)B3LYP-D3/6-31G(d)+SDD level of theory. The SOMO of an isobutyronitrile radical (–5.98 eV), which was generated through denitrogenation of AIBN, is closer to the HOMO level of Ni(II) norcorrole **1** (–4.68 eV) rather than its LUMO (–3.16 eV). This result explains the selective addition of the electrophilic isobutyronitrile radical to the distal α-position of the pyrrole unit. The calculated MO coefficient of the HOMO indicates that two α-carbons of the pyrrole subunits are the most reactive positions for electrophilic species. In addition, the distal α-carbon to the *meso* position could be more reactive than the proximal α-carbon due to the steric hindrance of bulky mesityl groups. Consequently, the isobutyronitrile radical predominantly attacks the distal α-carbon to the *meso* position to afford corresponding radical intermediate **I**. The calculated spin density of radical **I** revealed that **I-major** is a reactive resonance structure without steric effect from *meso*-substituents. Finally, another isobutyronitrile radical reacts with **I-major** from its convex face to form major product **2a** with two alkyl substituents on the same side of the molecule. For the byproducts, **3a** would be generated through the quenching of radical **I** with a hydrogen atom source. Bisdipyrrin **4a** could be formed through the ring opening reaction of **I** by the homolytic cleavage of the C(sp^2)–C(sp^2) bond to radical **II**, the addition of the isobutyronitrile radical, and subsequent demetallation.

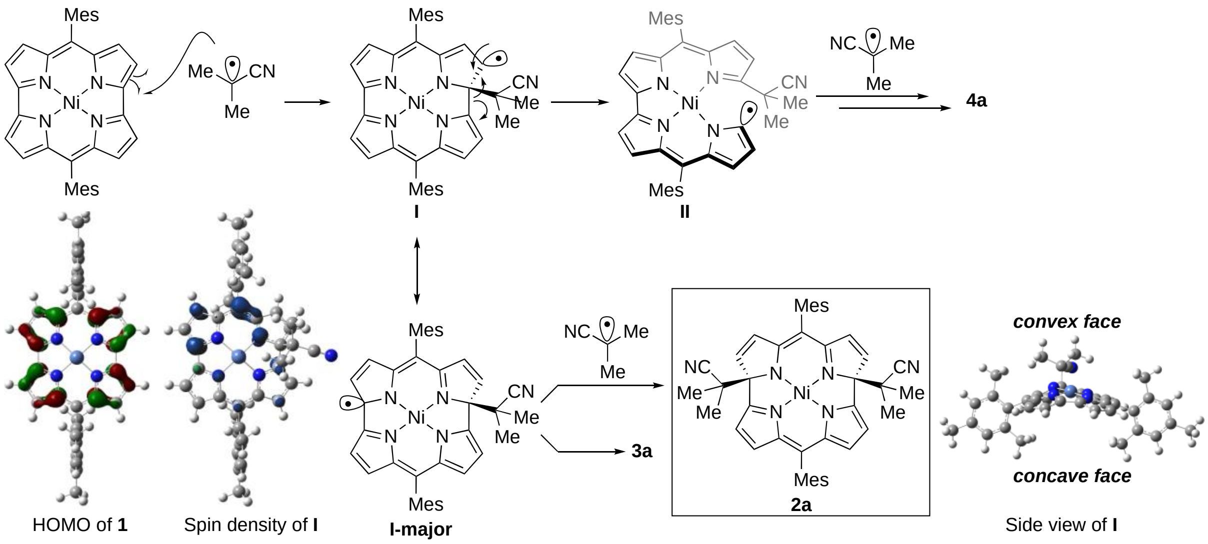

Scheme 3: Plausible reaction mechanism.

Conclusion

In conclusion, we have investigated the addition reaction of electrophilic alkyl radicals derived from azo radical initiators to antiaromatic Ni(II) norcorroles. The reaction smoothly proceeded to afford bowl-shaped non-conjugated macrocycles **2a** in excellent yields, which exhibited markedly different photophysical and electrochemical properties with norcorrole **1**. The intrinsic reactivities of Ni(II) norcorroles with neutral radical species were revealed by DFT calculations, where populations of the HOMO of the norcorrole unit and the spin density of the radical intermediate governed the regioselectivity.

Supporting Information

Supporting Information File 1: Experimental procedures, compound data with NMR and MS spectra, and the details of crystal data and DFT calculations.

File Name: Text

File Format: PDF

Funding

This work was supported by Japan Society for the Promotion of Science (JSPS) KAKENHI grants JP20H05863, JP22H04974, and JP22K19025. H. T. is grateful to the Ministry of Education, Culture, Sports, Science and Technology (MEXT) Leading Initiative for Excellent Young Researchers (Grant JPMXS0320220200) and the Foundation of Public Interest Tatematsu.

References

1. Bröring, M.; Köhler, S.; Kleeberg, C. *Angew. Chem. Int. Ed.* **2008**, *47*, 5658–5660.

2. Ito, T.; Hayashi, Y.; Shimizu, S.; Shin, J.-Y.; Kobayashi, N.; Shinokubo, H. *Angew. Chem. Int. Ed.* **2012**, *51*, 8542–8545.

3. Yonezawa, T.; Shafie, S. A.; Hiroto, S.; Shinokubo, H. *Angew. Chem. Int. Ed.* **2017**, *56*, 11822–11825.

4. Shin, J.-Y.; Yamada, T.; Yoshikawa, H.; Awaga, K.; Shinokubo, H. *Angew. Chem. Int. Ed.* **2014**, *53*, 3096–3101.

5. Ukai, S.; Fukui, N.; Ikeue, T.; Shinokubo, H. *Chem. Lett.* **2022**, *51*, 182–184.

6. Nozawa, R.; Tanaka, H.; Cha, W.-Y.; Hong, Y.; Hisaki, I.; Shimizu, S.; Shin, J.-Y.; Kowalczyk, T.; Irle, S.; Kim, D.; Shinokubo, H. *Nat. Commun.* **2016**, *7*, 13620.

7. Kawashima, H.; Ukai, S.; Nozawa, R.; Fukui, N.; Fitzsimmons, G.; Kowalczyk, T.; Fliegl, H.; Shinokubo, H. *J. Am. Chem. Soc.* **2021**, *143*, 10676–10685.

8. Kawashima, H.; Fukui, N.; Phung, Q. M.; Yanai, T.; Shinokubo, H. *Cell Rep. Phys. Sci.* **2022**, *3*, 101045.

9. Ishikawa, S.; Yamasumi, K.; Sugiura, S.; Sato, S.; Watanabe, G.; Koo, Y. H.; Seki, S.; Bando, Y.; Haketa, Y.; Shinokubo, H.; Maeda, H. *Chem. Sci.* **2024**. *Advance Article.* doi:10.1039/D4SC01633E

10. Kino, S.; Ukai, S.; Fukui, N.; Haruki, R.; Kumai, R.; Wang, Q.; Horike, S.; Phung, Q. M.; Sundholm, D.; Shinokubo, H. *J. Am. Chem. Soc.* **2024**, *146*, 9311–9317.

11. Li, S.; Sun, Y.; Meng, Y.; Li, X.; Zhang, S. *Chin. J. Org. Chem.* **2022**, *42*, 2390.

12. Nozawa, R.; Yamamoto, K.; Shin, J.-Y.; Hiroto, S.; Shinokubo, H. *Angew. Chem. Int. Ed.* **2015**, *54*, 8454–8457.

13. Liu, B.; Yoshida, T.; Li, X.; Stępień, M.; Shinokubo, H.; Chmielewski, P. J. *Angew. Chem. Int. Ed.* **2016**, *55*, 13142–13146.

14. Yoshida, T.; Shinokubo, H. *Mater. Chem. Front.* **2017**, *1*, 1853–1857.

15. Ren, D.; Fu, X.; Li, X.; Koniarz, S.; Chmielewski, P. J. *Org. Chem. Front.* **2019**, *6*, 2924–2933.

16. Deng, Z.; Li, X.; Stępień, M.; Chmielewski, P. J. *Chem. Eur. J.* **2016**, *22*, 4231–4246.

17. Kawashima, H.; Hiroto, S.; Shinokubo, H. *J. Org. Chem.* **2017**, *82*, 10425–10432.

18. Li, S.; Smaga, O.; Sun, Y.; Li, X.; Pawlicki, M.; Sukniewicz, M.; Chmielewski, P. J. *Org. Chem. Front.* **2021**, *8*, 3639–3652.

19. Liu, B.; Li, X.; Stępień, M.; Chmielewski, P. J. *Chem. Eur. J.* **2015**, *21*, 7790–7797.

20. Nozawa, R.; Yamamoto, K.; Hisaki, I.; Shin, J.-Y.; Shinokubo, H. *Chem. Commun.* **2016**, *52*, 7106–7109.

21. Fu, X.; Meng, Y.; Li, X.; Stępień, M.; Chmielewski, P. J. *Chem. Commun.* **2018**, *54*, 2510–2513.

22. Ren, D.; Smaga, O.; Fu, X.; Li, X.; Pawlicki, M.; Koniarz, S.; Chmielewski, P. J. *Org. Lett.* **2021**, *23*, 1032–1037.

23. Liu, S.-Y.; Tanaka, H.; Nozawa, R.; Fukui, N.; Shinokubo, H. *Chem. Eur. J.* **2019**, *25*, 7618–7622.

24. Shafie, S. A.; Kawashima, H.; Miyake, Y.; Shinokubo, H. *ChemPlusChem* **2019**, *84*, 623–626.

25. Fukuoka, T.; Uchida, K.; Sung, Y. M.; Shin, J.-Y.; Ishida, S.; Lim, J. M.; Hiroto, S.; Furukawa, K.; Kim, D.; Iwamoto, T.; Shinokubo, H. *Angew. Chem. Int. Ed.* **2014**, *53*, 1506–1509.

26. Liu, S.-Y.; Fukuoka, T.; Fukui, N.; Shin, J.-Y.; Shinokubo, H. *Org. Lett.* **2020**, *22*, 4400–4403.

27. Tabata, N.; Uchino, T.; Kitamura, C.; Yoshizawa, K.; Shiota, Y.; Kato, S. *Chem. Sci.* **2023**, *14*, 5974–5982.

28. Gaussian 16, Revision C.01, Frisch, M. J.; Trucks, G. W.; Schlegel, H. B.; Scuseria, G. E.; Robb, M. A.; Cheeseman, J. R.; Scalmani, G.; Barone, V.; Petersson, G. A.; Nakatsuji, H.; Li, X.; Caricato, M.; Marenich, A. V.; Bloino, J.; Janesko, B. G.; Gomperts, R.; Mennucci, B.; Hratchian, H. P.; Ortiz, J. V.; Izmaylov, A. F.; Sonnenberg, J. L.; Williams-Young, D.; Ding, F.; Lipparini, F.; Egidi, F.; Goings, J.; Peng, B.; Petrone, A.; Henderson, T.; Ranasinghe, D.; Zakrzewski, V. G.; Gao, J.; Rega, N.; Zheng, G.; Liang, W.; Hada, M.; Ehara, M.; Toyota, K.; Fukuda, R.; Hasegawa, J.; Ishida, M.; Nakajima, T.; Honda, Y.; Kitao, O.; Nakai, H.; Vreven, T.; Throssell, K.; Montgomery, J. A., Jr.; Peralta, J. E.; Ogliaro, F.; Bearpark, M. J.; Heyd, J. J.; Brothers, E. N.; Kudin, K. N.; Staroverov, V. N.; Keith, T. A.; Kobayashi, R.; Normand, J.; Raghavachari, K.; Rendell, A. P.; Burant, J. C.; Iyengar, S. S.; Tomasi, J.; Cossi, M.; Millam, J. M.; Klene, M.; Adamo, C.; Cammi, R.; Ochterski, J. W.; Martin, R. L.; Morokuma, K.; Farkas, O.; Foresman, J. B.; Fox, D. J. Gaussian, Inc., Wallingford CT, **2016**.